Quantum control of dissipative systems: Exact solutions

Jianshu Cao, Michael Messina, and Kent R. Wilson
Department of Chemistry and Biochemistry, University of California, San Diego, La Jolla, California 92093-0339

(Received 16 August 1996; accepted 11 October 1996)

Optimal quantum control theory, which predicts the tailored light fields that best drive a system to a desired target, is applied to the quantum dissipative dynamics of systems linearly coupled to a Gaussian bath. To calculate the material response function required for optimizing the light field, the analytical solution is derived for the two-level Brownian harmonic oscillator model and the recently developed method for directly simulating the Gaussian force is implemented for anharmonic Brownian oscillators. This study confirms the feasibility of quantum control in favorable condensed phase environments and explores new quantum control features in the presence of dissipation, including memory effects and temperature dependence. © *1997 American Institute of Physics.* [S0021-9606(97)51103-2]

I. INTRODUCTION: QUANTUM CONTROL OF DISSIPATIVE SYSTEMS

Recent theoretical and experimental progress in quantum control has demonstrated the possibility of driving matter toward a specific goal with tailored laser fields.[1–7] Theoretical tools[8–13] have been developed to predict an optimal laser field to drive a quantum wave packet to a desired functional form at a chosen time, and this type of quantum control has been experimentally realized in gas phase and condensed phase samplers and applied to the control of the products of a chemical reaction.[6,7,14–16] In the future we can expect to see further exploration of quantum control of more complicated and realistic systems, such as polyatomic molecules, clusters, solvated particles, crystals, etc. Theoretically, the challenge lies in the numerical difficulties of quantum dynamical calculations of many degrees-of-freedom systems. Various approximate approaches for wave packet propagation have been used to implement the equations of quantum control theory, including Gaussian wave packet (GWP),[17,18] time-dependent Hartree (TDH),[19] nearly classical (NC),[12,15,16] and stochastic bath (SB).[11] Although a start has been made, the quantum control of dissipative systems has not been analyzed in a fully systematic and rigorous fashion. In this paper, a condensed phase system is reduced to a one-dimensional system which represents the degree of freedom associated with the target and a Gaussian bath which includes the infinite degrees of freedom of the environment. Although simplified, this stochastic model can be solved accurately and the results thus obtained characterize the general properties of condensed phase quantum control.

To begin, we briefly review the theoretical formulation of an optimal weak control field for driving a dissipative molecule to a desired target. Although most results here have been given previously,[8,11–13,20,21] the emphasis of this section is the formulation of weak optical field control of dissipative systems.

Consider a molecule coupled to a time-dependent electric field via a dipole interaction. For simplicity, the molecular system consists of two electronic states, a ground state $|g\rangle$ and an excited state $|e\rangle$, described by two diabatic Hamiltonians, H_g and $(H_e+\hbar\omega_{eg})$, respectively. The electric field is treated classically as

$$\epsilon(t)=E(t)e^{-i\omega_{eg}t}+E^*(t)e^{i\omega_{eg}t}, \tag{1.1}$$

with ω_{eg} being the transition frequency between the two electronic states, which is assumed to be much larger than the vibrational energy spacings. Within the rotating wave approximation, the coupled matter and field Hamiltonian is given by

$$H(t)=H_M+H_{\rm int}, \tag{1.2}$$

where the molecular term is $H_M=H_g|g\rangle\langle g|+H_e|e\rangle\langle e|$ and the interaction term is $H_{\rm int}=-\mu E(t)|g\rangle\langle e|-\mu E^*(t)|e\rangle\langle g|$, with μ being the transition dipole moment. The density matrix of the molecular system obeys the Liouville equation of motion

$$\frac{d\rho(t)}{dt}=-\frac{i}{\hbar}[H(t),\rho(t)]=-i\mathscr{L}(t)\rho(t), \tag{1.3}$$

where $\mathscr{L}$ is the Liouville operator. The evolution of the density matrix $\rho(t)$ as described by the above equation contains all the information about the system.

In general, the target of quantum control can be specified as an operator A and the degree of control is measured by the expectation value of this target operator at time t_f,[12] or explicitly,

$$A(t_f)=\mathrm{Tr}[A\rho(t_f)]. \tag{1.4}$$

In the weak response regime, the analysis is simplified by linearizing the Liouville operator in terms of the field. Assume that the initial density matrix is defined on the ground state, ρ_g, and the target operator is defined on the excited state, A_e; then the leading term of the expectation value of the target is[12]

$$A(t_f)=\int_0^{t_f}dt\int_0^{t_f}dt'E^*(t)M(t,t')E(t'), \tag{1.5}$$

where the material response function matrix M is defined as

$$M(t,t')=\frac{1}{\hbar^2}\ \mathrm{Tr}[A_e e^{-iH_e(t_f-t')}\mu e^{-iH_g t'}\rho_g e^{iH_g t}\times\mu e^{iH_e(t_f-t)}]. \tag{1.6}$$

The goal is to find an external field $E(t)$ which maximizes the realization of such a target under certain constraints. To this end, we construct a functional as

$$J(t_f)=A(t_f)-\lambda\int_0^{t_f}|E(t)|^2dt, \tag{1.7}$$

where the Lagrange multiplier λ is introduced to lift the constraint on the total radiation energy. Rigorously, the optimization of the field can be achieved by a variational differentiation of the functional $J(t_f)$ with respect to the field, $\delta J(t_f)/\delta E^*(t)=0$. In the weak response regime, application of the variational procedure results in a linear field equation

$$\lambda E(t)=\int_0^{t_f}M(t,t')E(t')dt', \tag{1.8}$$

which can be solved as a conventional eigenvalue problem.

A yield function,[12] a measure of how well the goal is reached,

$$y=\frac{A(t_f)}{\int_0^{t_f}|E(t)|^2dt}, \tag{1.9}$$

is introduced, which has the same value as the eigenvalue λ when evaluated for the optimized field computed from Eq. (1.8). This is the expectation value of the target per molecular per unit incident pulse energy. It then follows that for a given molecular system and a given target, the eigenvector corresponding to the largest eigenvalue is the globally optimal field which achieves the maximum yield relative to any nonoptimized pulses with the same pulse energy.[12]

The above formulation in Liouville space is applicable to many-body systems, mixed states, thermal canonical ensembles, providing sufficient flexibility to include a broad range of experimental considerations.[11] In particular, the solvent influences on wavepacket focusing in the condensed phase can be investigated within this framework. In practice, an interesting scenario is to define a target on the degree of freedom of interest so that only the dynamics projected onto this reduced space is relevant and the dynamics of the orthogonal space is treated as dissipation. In other words, dissipation arises from the coupling of a system to an infinite number of degrees of freedom of a bath, which results in time irreversible dynamics of the system. It is interesting and useful to examine the effects of such irreversible dynamics on wavepacket focusing.

The major challenge to such a many-atom study lies in the numerical implementation of quantum control theory for dissipative systems, because the difficulty of quantum dynamics calculations increases enormously with dimensionality.[22–27] Accurate methods, such as basis set expansions and path integral calculations of real time correlation functions, are limited to a few degrees of freedom and short time dynamics, and are thus incapable of treating dissipation in more general situations. An accurate and general numerical algorithm for simulating quantum dissipation is not now available, nor is it expected in the near future. Therefore, a linearized quantum dissipation model, termed the Gaussian bath model, has become the subject of many analytical[28–31] and numerical[32–36] studies.

The Gaussian bath model consists of a system degree-of-freedom q and N linear harmonic oscillators $\{x_i\}$, described by the Hamiltonian

$$H=\frac{1}{2}m\dot{q}^2+V(q)+\sum_{i=1}^{N}\frac{1}{2}m_i\dot{x}_i^2+\frac{1}{2}m_i\omega_i^2\left(x_i-\frac{c_i}{m_i\omega_i^2}q\right)^2, \tag{1.10}$$

where $V(q)$ is the potential as a function of q,x_i is the ith Gaussian bath normal mode, m_i is the mass, ω_i is the harmonic frequency, and c_i is the coupling strength. It was shown by Zwanzig[28] that the elimination of the bath modes from the equations of motion for the above Hamiltonian yields the generalized Langevin equation (GLE)

$$m\ddot{q}(t)+\frac{d}{dq}V[q(t)]+\int_0^t\eta(t-t')\dot{q}(t')dt'=F(t), \tag{1.11}$$

where $F(t)$ is the random force and m is the mass of the quantum particle. The dynamical friction coefficient $\eta(t)$ is then identified as

$$\eta(t)=\sum_{i=1}^{N}\frac{c_i^2}{m_i\omega_i^2}\cos(\omega_i t)=\frac{2}{\pi}\int_0^\infty d\omega\frac{J(\omega)}{\omega}\cos(\omega t), \tag{1.12}$$

where $J(\omega)$ is the spectral density, defined in the discrete limit by

$$J(\omega)=\frac{\pi}{2}\sum_{i=1}^{N}\frac{c_i^2}{m_i\omega_i}\delta(\omega-\omega_i). \tag{1.13}$$

The random force can be explicitly expressed in terms of the initial conditions of the bath variables. Therefore, under the assumption that the initial bath distribution in phase space is in thermal equilibrium in the presence of the system, one can show that

$$\eta(t)=\beta\langle F(t)F(0)\rangle, \tag{1.14}$$

where the equilibrium condition $\langle F\rangle=0$ is implied. The introduction of the spectral density $J(\omega)$ makes it possible to pass from a discrete set of modes to a continuum spectrum, and hence to represent an arbitrary time-dependent friction $\eta(t)$. The relation in Eq. (1.14) holds for a Gaussian bath regardless of the form of the potential of mean force. It is for this reason that the Gaussian bath is an attractive analytical model to study the solvent frictional effects on vibrational relaxation and activated reaction dynamics.

The Gaussian bath can be easily quantized to represent quantum dissipation and thereby can serve as a prototype for

formulating quantum Brownian motion, dissipative tunneling, solvent-induced electron transfer, and other quantum processes in the condensed phase. It is therefore the focus of this paper to calculate the material response function of a quantum system which is linearly coupled to a Gaussian bath.[11] To this end, the analytical solution of the Brownian oscillator is derived in Sec. II and the simulation scheme of dissipative systems proposed by Cao, Ungar, and Voth[36] is reviewed in Sec. III. Results based on these two methods are presented in Sec IV and a discussion in Sec. V concludes the paper.

II. A SOLVABLE MODEL: THE TWO-LEVEL BROWNIAN OSCILLATOR SYSTEM

One of the well-studied analytical models is the displaced two-level Brownian oscillator system, which has been solved semi-classically by Yan and Mukamel[37] and quantum mechanically by Tanimura and Mukamel.[38] Our derivation of the quantum propagator of the displaced Brownian oscillator sketched in Appendix A is both mathematically simple and physically intuitive. This result has recently been used to rederive the Marcus's electron transfer rate formula based on the exact electronic dynamics.[39] Quantum control with such a model has previously been studied by Yan *et al*[11] semiclassically and will be further investigated in this section with the help of the quantum propagator.

The two-level Brownian oscillator model has been popularized as a primary analytically solvable model to describe the electronic absorption line shape and various nonlinear spectra in condensed phases.[37,38,40] In this model, both the molecular system and the thermal bath consist of harmonic oscillators:

$$H_e=\tfrac{1}{2}m\dot{q}^2+\tfrac{1}{2}m\omega_0^2q^2, \tag{2.1}$$

$$H_g=\tfrac{1}{2}m\dot{q}^2+\tfrac{1}{2}m\omega_0^2(q-d)^2, \tag{2.2}$$

and

$$H=H_g|g\rangle\langle g|+H_e|e\rangle\langle e| +\sum_{i=1}^{N}\left[\frac{m_i\dot{x}_i^2}{2}+\frac{m_i\omega_i^2}{2}\left(x_i-\frac{c_i}{m_i\omega_i^2}q\right)^2\right]. \tag{2.3}$$

Here, q is the Brownian oscillator coordinate, with its bare frequency ω_0 and harmonic displacement d, and the set $\{x_i\}$ constitutes the bath modes, with frequencies $\{\omega_i\}$, masses $\{m_i\}$, and coupling constants $\{c_i\}$. In Appendix A, we illustrate that the quantum propagator of the Brownian oscillator defined above can be solved in a closed form, which is most conveniently expressed in Wigner phase space as in Eq. (A8).

To obtain an analytical expression for the response function, we assume a Gaussian target in the excited electronic state, defined in the Wigner phase space representation as

$$A_e(q,p)=\frac{1}{2\pi\sqrt{W_qW_p}}\ \exp\left[-\frac{(q-q_c)^2}{2W_q}-\frac{(p-p_c)^2}{2W_p}\right], \tag{2.4}$$

where q_c and p_c represent the center of the target in phase space, with W_q and W_p being the widths of the target. Then, given Eq. (A 8) and assuming a constant transition dipole moment $\mu=1$, the material response function is expressed as

$$M(t,t')=\frac{1}{2\pi\sqrt{(W_q+\langle q^2\rangle)(W_p+\langle p^2\rangle)}} \times\exp\left[-\frac{(q_c+d-\overline{q(t_f)})^2}{2(W_q+\langle q^2\rangle)}-\frac{(p_c-\overline{p(t_f)})^2}{2(W_p+\langle p^2\rangle)}+\frac{i\phi}{\hbar}\right]. \tag{2.5}$$

Here, the dynamical parameters $\overline{q(t)},\overline{p(t)}$, and ϕ as defined by Eqs. (A9)–(A11) and the equilibrium parameters $\langle q^2\rangle$ and $\langle p^2\rangle$ as defined by Eqs. (A14) and (A15) will be specified for the material response function in the following.

To start, the potential difference of the Hamiltonian in Eq. (2.3) of the displaced harmonic oscillator is

$$H'=H_e-H_g=-fx+\tfrac{1}{2}fd, \tag{2.6}$$

with $f=m\omega_0^2d$. According to the definition of the material response function, the time-dependent potential difference in Eq. (A2) is determined in a piecewise fashion by $f_+(t)=f_-(t)=U_-(t)=0$, if $0\leqslant t\leqslant t_1$; $f_+(t)=f_-(t)=f$, $U_-=fd/2$, if $t_1<t\leqslant t_2$; and $f_+(t)=2f, f_-(t)=U_-(t)=0$, if $t_2<t\leqslant t_f$. Then the dynamical parameters defined in the Eq. (A9)–(A11) can be explicitly written as

$$\overline{q(t_f)}=\frac{f}{2\pi}\int d\omega\ \frac{\mathrm{Im}\ \chi}{\omega}\{2-\cos(\omega t_1')-\cos(\omega t_2') +i\ \coth(b/2)[\sin(\omega t_1')-\sin(\omega t_2')]\}, \tag{2.7}$$

$$\overline{p(t_f)}=\frac{mf}{2\pi}\int d\omega\ \frac{\mathrm{Im}\ \chi}{\omega}\{\sin(\omega t_1')+\sin(\omega t_2') +i\ \coth(b/2)[\cos(\omega t_1')-\cos(\omega t_2')]\}, \tag{2.8}$$

and

$$\phi(t_f)=\frac{f^2}{2\pi}\int d\omega\ \frac{\mathrm{Im}\ \chi}{\omega^2}\{i\ \coth(b/2) \times[1-\cos\ \omega(t_2-t_1)]-\sin\omega(t_2-t_1)]\}, \tag{2.9}$$

where $t_1'=t_f-t_1, t_2'=t_f-t_2$, and Im χ is the imaginary part of the linear response function.

For an exponential decay frictional kernel defined as

$$\eta=\eta_0De^{-Dt}, \tag{2.10}$$

with D being the decay constant and η_0 being the friction strength, the linear response function in Eq. (A18) becomes

$$\chi(\omega)=\frac{1}{m(\omega_0^2-\omega^2)-i\omega\eta_0D/(D-i\omega)}, \tag{2.11}$$

which in the limit of $D\to\infty$ reduces to the response function of an Ohmic friction. Given the Laplace transformation of the friction kernel $\tilde{\eta}(s)=\eta_0D/(D+s)$, the equilibrium parameters $\langle q^2\rangle$ and $\langle p^2\rangle$ defined in Eqs. (A14) and (A15) can be evaluated numerically.

Previously, within the framework of semi-classical propagation, Yan *et al.*[11] have calculated the globally optimal fields and the corresponding yield for the same Hamiltonian as in Eq. (2.3). Apparently because of the nature of the semi-classical approximation, their expression of the material response function in Eq. (60) of Yan *et al.*[11] differs from the exact expression in Eq. (2.5) in the following two aspects. The Gaussian width given as $\overline{n+1/2}$ by Yan *et al.*[11] does not include the dissipation effects as in the definitions of $\langle q^2\rangle$ and $\langle p^2\rangle$ given by Eqs. (A14) and (A15). Also, the Gaussian bath given by Yan *et al.*[11] is not fully quantized as in Eq. (A 16). Nevertheless, at least qualitatively, their conclusions derived from the semi-classical formula agree well with our analysis.

III. DIRECT SIMULATION OF DISSIPATIVE DYNAMICS

Our algorithm for calculating the material response functions for dissipative systems is based on a novel simulation method published recently.[36] The approach is derived from a very simple idea: since the bath actions are quadratic and thus the functional integrand of the Gaussian bath in the discretized form is a multidimensional complex Gaussian function, the bath average can be carried out by direct Monte Carlo sampling. Given a bath path generated by the Gaussians, the system can be propagated under the influence of the time-dependent fluctuating bath force through any method of choice, such as matrix or tensor multiplication,[35,41] split operator propagation,[42] wave packet dynamics,[43,44] semi-classical propagation,[45,46] centroid molecular dynamics,[47] etc. Averaging the time-dependent system quantities over the bath variables yields the desired physical quantities of the quantum system-bath Hamiltonian. This procedure thus provides a large array of possibilities for simulating quantum dynamical evolution of dissipative systems.

To begin, the Hamiltonian in Eq. (2.3) is rewritten as

$$H=H_b(x)+V_c(x,q)+H_s(q), \tag{3.1}$$

where $H_b(x)$ is the bath Hamiltonian

$$H_b=\sum_{i=1}^{N}\left[\frac{p_i^2}{2m_i}+\frac{1}{2}m_i\omega_i^2x_i^2\right], \tag{3.2}$$

$V_c(x,q)$ is the coupling potential

$$V_c(x,q)=-\sum_{i=1}^{N}c_ix_iq, \tag{3.3}$$

and $H_s(q)$ is the system Hamiltonian

$$H_s(q)=H_g|g\rangle\langle g|+H_e|e\rangle\langle e|+\sum_{i=1}^{N}\frac{c_i^2}{2m_i\omega_i^2}q^2, \tag{3.4}$$

with the last term being the counter potential.

Assuming the physical quantity of interest F is a function of the system variables only, one can then express this quantity in terms of a bath average defined as (the index i for bath variables implied)

$$\langle F[x_f(t),x_b(t),x_\beta(\tau)]\rangle_b=\frac{\int dx_1\,dx_2\,dx_3\int\mathscr{D}x_f(t)\mathscr{D}x_b(t)\mathscr{D}x_\beta(\tau)F[x_f(t),x_b(t),x_\beta(\tau)]e^{-\overline{S}/\hbar}}{\int dx_1\,dx_2\,dx_3\int\mathscr{D}x_f(t)\mathscr{D}x_b(t)\mathscr{D}x_\beta(\tau)e^{-\overline{S}/\hbar}}. \tag{3.5}$$

Here, $\overline{S}$ is the summation of actions evaluated along the closed path, explicitly given as

$$\overline{S}=S_\beta[x_\beta(\tau)]-iS[x_f(t)]+iS[x_b(t)], \tag{3.6}$$

where $S[x_f(t)]$ is the real time action functional for the forward path $x_f(t)$,$S[x_b(t)]$ is the real time action functional for the backward path $x_b(t)$, and $S_\beta[x(\tau)]$ is the imaginary time action functional for the thermal path $x_\beta(\tau)$. In addition, the bath configuration is understood as follows: $x_f(t)$ is the forward path satisfying the boundary conditions $x_f(0)=x_1$ and $x_f(t_f)=x_3$,$x_b(t)$ is the backward path satisfying the boundary conditions $x_b(0)=x_2$ and $x_b(t_f)=x_3$, and $x_\beta(\tau)$ is the imaginary time path satisfying the boundary conditions $x_\beta(0)=x_1$ and $x_\beta(\hbar\beta)=x_2$, so that a closed trace path is formed for the thermal averaged real time propagation for $t=0$ to $t=t_f$ at temperature β.

With the introduction of the bath average, the formal expression of a physical quantity of the system can be simplified enormously. In particular, the material response function of Eq. (1.6) is now expressed as (setting $\mu=1$)

$$\begin{aligned}M(t,t')=\frac{1}{\hbar^2}\langle\mathrm{Tr}[&A_e\,e^{-i\int_t^{t_f}H_e[q,x_f(t)]\,dt/\hbar}\\&\times e^{-i\int_0{}_tH_g[q,x_f(t)]\,dt/\hbar}\rho_g\,e^{i\int_{t'}^{t_f}H_g[q,x_b(t)]\,dt/\hbar}\\&\times e^{-i\int_0{}_{t'}H_e[q,x_b(t)]\,dt/\hbar}A_b\rangle,\end{aligned} \tag{3.7}$$

where the operators A and ρ_g are evaluated at the final time t_f and the initial time 0, respectively. In the above equation, $H[q,x_f(t)]=H_q(q)+V_c[x_f(t),q]$ and $H[q,x_b(t)]=H_q(q)+V_c[x_b(t),q]$ are the time-dependent system Hamiltonians evolving under the influence of the Gaussian force, the Tr symbol denotes a trace over the system variables, and the exponential operators are understood as being time-ordered products.

As has been argued, the quadratic functional in Eq. (3.2) can be diagonalized, giving rise to Gaussian functionals with complex eigenvalues and through a coordinate rotation the bath average can be sampled by the direct Monte Carlo method. The details of the diagonalization and coordinate rotation are explained by Cao *et al.*[36] and in Appendix B.

For our purpose, the material response function as expressed by Eq. (3.7) is evaluated through the split operator propagation with the help of the fast Fourier transform (FFT). In the case that the target is a pure state, it is beneficial to propagate the target wave function backward in time because the dimension of a wave function is half the dimension of the corresponding density matrix.

With the above development in hand, we can simulate the dynamics of a quantum system interacting with a Gaussian bath. The procedure is described as follows:

(1) Choose a finite set of linear harmonic oscillators to represent the Gaussian bath. Care must be taken to avoid nonergodicity of the bath for the time period of interest.
(2) For each mode, sample the three terminal points according to Eq. (B2) and generate the three paths according to Eq. (B9). The quantum fluctuating force is the superposition of the contributions from all modes.
(3) The quantum system is propagated under the influence of the time-dependent complex quantum force, and the quantity of interest is computed.
(4) Steps (2) and (3) are repeated for many independent bath configurations. The bath averaged quantity represents the quantum dynamical measurement under the dissipative environment.

IV. RESULTS AND DISCUSSION

The methods described in the previous two sections make it possible to thoroughly investigate the various factors present in the quantum control of condensed phase systems, such as temperature, friction, and memory effects. The analytical solution of the Brownian oscillator is used to demonstrate the feasibility of control under condensed phase conditions, while the numerical calculation of a dissipative anharmonic oscillator is used to predict characteristic changes in the globally optimal field introduced by the condensed phase environment.

The first example is the two-level Brownian oscillator defined by Eq. (2.3) with parameters assigned as $m=1,\hbar=1,\omega_0=1,d=5$. The target is set at $q_c=5,p_c=0$, and $t_f=5$ with Gaussian widths $W_q=0.5$ and $W_p=0.5$. The dynamical friction kernel assumes the form of an exponential decay function as defined in Eq. (2.10) with $D=1$ for non-Ohmic friction and $D=\infty$ for Ohmic friction. First, the material response function was evaluated according to Eq. (2.5) on a time grid with a time discretization of 0.1. The discretized material response matrix was then diagonalized giving the yield as the maximum eigenvalue and the globally optimal field as the corresponding eigenvector.

In Fig. 1, the quantum yield defined by Eq. (1.9) is plotted as a function of the friction strength η_0 for Ohmic and non-Ohmic friction at an inverse temperature $\beta=1$. While both curves show the dramatic decrease of the yield because of the increase in friction, the non-Ohmic dissipative system clearly has a higher yield than the Ohmic dissipative system. This enhancement of the yield is due to memory effects. Since an oscillator interacts with the environment dynamically only through the resonant mode of the bath, the effective friction strength of non-Ohmic friction is much smaller than that of Ohmic friction, although the integrated friction strength η_0 is the same.

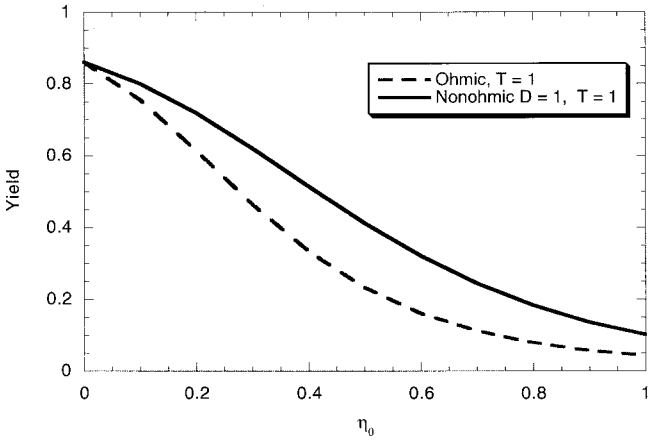

FIG. 1. The quantum yield, Eq. (1.9), of the Brownian oscillator defined by Eq. (2.3) as a function of the friction strength η_0 for Ohmic and non-Ohmic frictions at $\beta=1$. The friction kernel assumes the form of exponential decay as defined by Eq. (2.10) with $D=\infty$ for Ohmic friction and $D=1$ for non-Ohmic friction.

The above calculation of the quantum yield in the presence of dissipation is significantly underestimated for the following reasons. First, the width of the Brownian oscillator $\langle q^2\rangle$ in coordinate space decreases with friction strength, whereas its width $\langle p^2\rangle$ in momentum space increases with friction strength. Consequently, a minimum uncertainty wavepacket with $W_q=W_p=0.5$ is no longer a reasonable target when thermal fluctuations and dissipation are present. It is evident from Eq. (A14) that the spatial spreading of the Brownian oscillator $\langle q^2\rangle$ decreases with the friction η_0 and this decrease is much more significant at low temperature than at high temperature where the thermal spreading becomes dominant.

Second, a well-focused wave packet moves along a very different trajectory in phase space rather than a dissipative wavepacket. According to our previous model analysis,[21] the center of a focused wave packet in a nondissipative system obeys the classical equation of motion such that its trajectory lies on a constant energy surface in phase space. In the presence of dissipation, the initially excited system will lose energy while approaching thermal equilibrium. Therefore, a reasonable target for a conserved system, which satisfies the energy conservation law, will become difficult to achieve for a dissipative system, and the optimal light field for a dissipative system will need to impart more initial energy to a wavepacket than the target energy, as has been observed in previous nearly classical control simulations.[12] As an example, the quantum yield is plotted in Fig. 2 as a function of the target momentum p_c at a fixed target position $q_c=4$ at zero temperature for the displaced oscillator described earlier. For the simple displaced oscillator, two peaks at $p_c=\pm 3$ are observed, as expected from energy conservation. However, with a friction of the form of Eq. (1.10) with

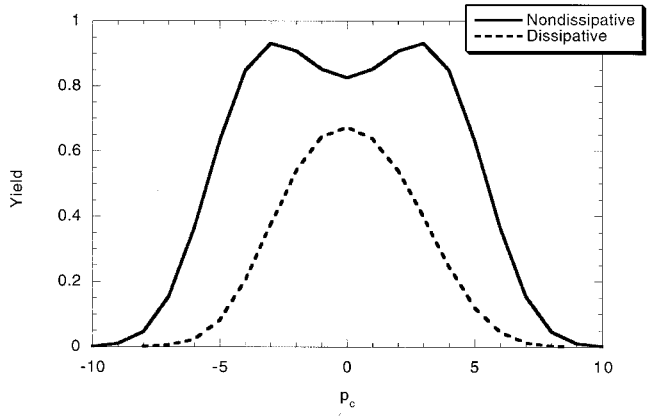

FIG. 2. The quantum yield, Eq. (1.9), as a function of the target momentum p_c for the same dissipative and nondissipative Brownian oscillators as described for Fig. 1. The spatial center of the target wave function is fixed at $q_c=3$.

an exponential decay kernel of $D=1$ and $\eta_0=0.5$, the maximum yield is achieved with zero momentum. In fact, for this Brownian oscillator, so much energy has been lost to the bath that the center of the wavepacket can no longer reach the target.

For the second example, to demonstrate dissipative effects on the globally optimal field, we employ a quartic potential for the excited state,

$$V_e=\tfrac{1}{2}x^2+\theta(x)gx^4, \tag{4.1}$$

with $g=-0.003$ and a displaced harmonic potential for the ground state

$$V_g=\tfrac{1}{2}(x+d)^2, \tag{4.2}$$

with $d=5$. Here, the Heaviside function is defined as $\theta(x)=1$ for $x\geqslant 0$ and $\theta(x)=0$ for $x<0$, and again unit values are assumed for mass, frequency, and the Planck constant. The system is initially in thermal equilibrium on the ground electronic state. The target wave function is a minimum uncertainty wavepacket $A=|\phi_f\rangle\langle\phi_f|$ on the excited electronic state at $q_c=5$ and $p_c=-2$, and the target time is $t_f=5$. The dissipation assumes the exponential decay form as in Eq. (2.10) with $\eta_0=0.1$ and $D=1.0$.

As described earlier, the direct Monte Carlo sampling of the Gaussian force can be incorporated into the computation of the material response function defined in Eq. (3.7). In order to reproduce the bath fluctuations as the time of interest, 20 harmonic oscillators were employed with frequencies evenly distributed from $\omega=0$ to $\omega=5$. The target wave function was propagated backward under the complex bath force through the split operator method with a time step of 0.1 and a spatial grid of 128 points. When at $t=0$, both the target wave function and its corresponding complex conjugate were integrated with the ground state density matrix ρ_g in coordinate space. This procedure was averaged over 10^4 independent bath configurations to reach convergence of the material response function.

The optimal fields computed from Eq. (1.8) are then represented in the Wigner transformation[12] defined as

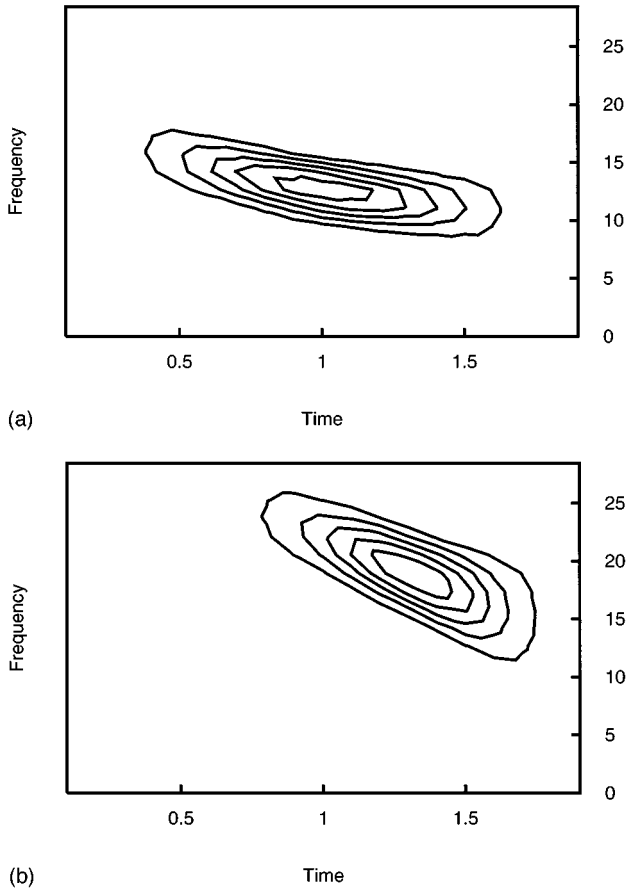

FIG. 3. Contour plots of the Wigner transformations of the optimal fields for the anharmonic oscillator Eq. (4.1) at $\beta=\infty$, without friction (a) and with exponential decay friction (b).

$$F(t,\omega)=\int_{-\infty}^{\infty} d\tau e^{-i\omega\tau}E^*(t+\tau/2)E(t-\tau/2), \tag{4.3}$$

which reduces to the power spectrum $|E(\omega)|^2$ when integrated over the time variable and reduces to the temporal field strength $|E(t)|^2$ when integrated over the frequency variable. Roughly speaking, the slope on the $F(t,\omega)$ contour diagram, defined as the tangent formed by the time axis and the principle axis of the contour rotated from the time axis, is proportional to the linear chirp rate.[21]

The contour plots of the Wigner transformations of the optimal fields at zero temperature are compared for the nondissipative anharmonic oscillator in Fig. 3(a) and for the dissipative anharmonic oscillator in Fig. 3(b). As can be seen from the results, once dissipation is introduced, the carrier frequency increases, the linear chirp rate increases, and the time between the excitation and the target is shortened. These effects have been observed in a earlier nearly classical simulation of the optimal quantum control of I_2 photodissociation in liquid density argon.[12,48] Clearly, the increase of the carrier frequency is the consequence of energy loss to the bath, and the decrease of the travel time of the wavepacket is the result of the lowering of the position of the outer turning point due to the dissipation. The change in the linear chirp

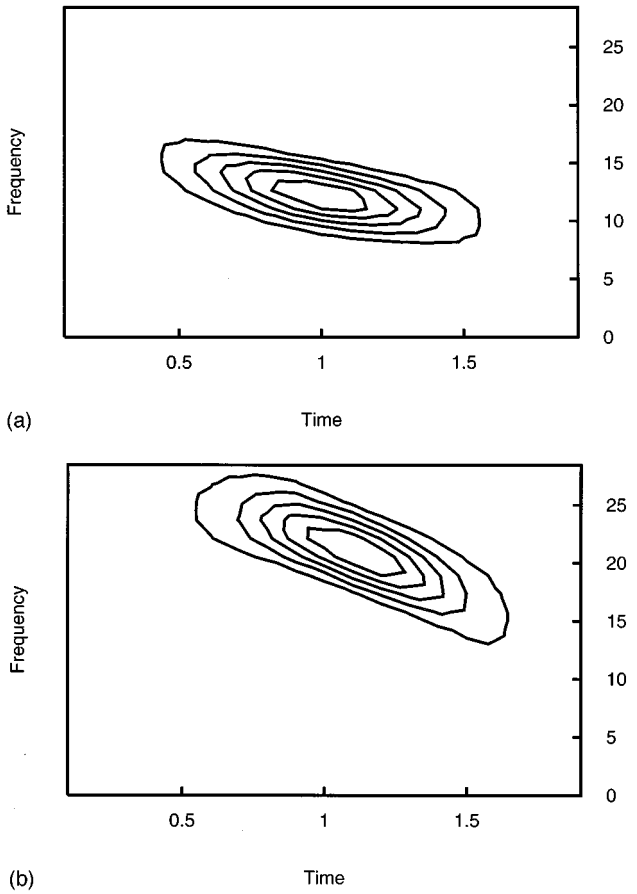

FIG. 4. The same plots of the Wigner transformations of the optimal fields as described for Fig. 3 except for at $\beta=1$, without friction (a) and with exponential decay friction (b).

rate can be explained from the point of view of energy relaxation. As demonstrated in a previous paper,[21] the chirp required to focus a wave packet is directly proportional to the energy dispersion, which changes as a consequence of dissipation.

It is interesting to note that some of the dissipative effects described above have also been observed in the calculations of a two-dimensional system, i.e, a system degree of freedom plus a harmonic oscillator.[19] It should be pointed out, however, that we attribute the changes in the optimal fields to the dissipative effects instead of to caging effects since, by use of the counter potential term of Eq. (1.10), the caging phenomena commonly found in solutions is not presented in the potential of mean force $V(q)$. In the paper by Messina,[19] the time-dependent Hartree approximation is shown to be of sufficient accuracy for the control period, indicating the possibilities that this approximation may be appropriate for larger systems. The numerical results of these simulations also suggest that some control may survive over a short time period in the presence of relatively strong dissipation.

Finally, Fig. 4 is the contour plot of the Wigner transformation of the optimal field at $\beta=1$ to be compared with Fig. 3 of the same plot at $\beta=\infty$. Clearly, when the temperature is raised, the optimal field for the dissipative oscillator changes significantly, whereas the optimal field for the nondissipative oscillator remains virtually the same. As argued before,[11] a nondissipative system at nonzero temperatures can be treated as a weighted superposition of energy eigenstates. Thus, the optimization procedure leads to the maximization of the quantum yield for the most populated energy eigenstate while ignoring the other states. Consequently, the optimal field of a nondissipative system has a weak dependence on temperature. However, the above argument is invalid for the dissipative system because the wave function description is incapable of including relaxation, in particular pure dephasing. In fact, the evolution of the density matrix is strongly influenced by the dissipation, which in turn depends strongly on temperature. As a result, the optimal field for a dissipative system changes drastically with temperature.

V. CONCLUSIONS

In this paper, the optimal control fields of two dissipative systems are solved exactly. the results not only confirm the findings in previous papers[11,15–17] but also provide new insight into the feasibility and characteristics of quantum control in condensed phases. In summary, the following conclusions can be drawn based on our case studies:

(1) Although dissipation reduces the quantum yield, the globally optimal field can still lead to a significant amount of control of the dissipative system. The quantity of control depends on the strength of the friction as well as the functional form of the memory kernel. A non-Ohmic bath results in higher quantum yields than an Ohmic bath at the same integrated strength.
(2) In general, quantum yields also depend on the desired target, since targets which are reachable on classical trajectories are more achievable. Since the equilibrium and dynamical properties of dissipative systems are different from those of conserved systems, the target wave function should be modified accordingly, if higher yield is desired.
(3) Dissipative effects on the globally optimal fields are observed: increase in carrier frequency, increase in linear chirp rate, shortening in pulse duration, and broadening in bandwidth, confirming the conclusions of earlier Gaussian wave packet (GWP),[17,18] time-dependent Hartree (TDH),[19] nearly classical (NC)[12,15,16] and stochastic bath (SB)[11] simulations.
(4) Temperature effects on globally optimal fields are more drastic for dissipative systems than for nondissipative systems.

It remains a question how well a stochastic model based on the generalized Langevin equation in Eq. (1.11) can describe a condensed phase environment and how a realistic spectral density can be obtained which best represents the environment. From a simplistic point of view, as long as the total system can be divided into a bath and a reduced system, such that the effects of the bath result in irreversible dynam-

ics of the reduced system and the effects of the reduced degrees of freedom on the bath dynamics are negligible, this stochastic view of many-body dynamics is justified. Meanwhile, from a practical point of view, if the generalized Langevin dynamics with a friction kernel calculated from the fluctuation-dissipation relation Eq. (1.14) reproduces the physical quantities of interest, the accuracy of the Gaussian bath model is verified. Following this line, we have recently performed classical dynamics simulations of excited iodine molecules in argon matrices and have confirmed the Gaussian bath model based on a coordinate dependent friction kernel computed from force–force correlation functions. It would be interesting to carry out a full quantum dissipative simulation and to solve for the globally optimal control field.

APPENDIX A: PROPAGATION OF A TWO-LEVEL BROWNIAN OSCILLATOR

In this section, we will derive the quantum propagator of a two-level Brownian oscillator in Liouville space. The final result is the same as the Liouville space generation functional introduced by Mukamel and co-workers,[37,38] and has been applied to a wide range of problems. However, the derivation presented here is simple in mathematical derivation and intuitive in physical reasoning.

To begin, we assume thermal equilibrium on one of the diabatic states and define the difference of the two diabatic surfaces as

$$\hat{H}' = -f\hat{q} + U, \tag{A1}$$

where U is the difference of potential energies and f is the difference of force constants. The propagation of the two-level Brownian oscillator can be written as

$$\hat{G}(t) = \sum_{n=0}^{\infty} (-i)^n \left(\frac{\Delta}{\hbar}\right)^n \times \int_0^t dt_n \int_0^{t_n} dt_{n-1} \int_0^{t_{n-1}} dt_{n-2} \cdots \int_0^{t_2} dt_1 \times \exp\left\{ -i \int_0^t [\hat{H}_0 + \hat{H}'(t')]/\hbar \; dt' \right\}, \tag{A2}$$

where the time-dependent function $H'(t')$ is defined in piecewise fashion as $H'(t') = H'$ for $t_{2l} < t' < t_{2l+1}$ and $H'(t') = 0$ for $t_{2l-1} < t' < t_{2l}$. The central quantity is the propagator of a forced harmonic oscillator, which in terms of the density matrix is given by

$$\hat{\rho}(t) = \exp\left[-i \int_0^t \hat{H}_L(t')/\hbar dt' \right] \hat{\rho}_{eq} \times \exp\left[i \int_0^t \hat{H}_R(t')/\hbar dt' \right] = \hat{G}_L(t) \hat{\rho}_{eq} \hat{G}_R(t), \tag{A3}$$

with the subscripts L and R denoting forward and backward propagations, or, left and right propagations, respectively.

To start, considering a frictionless harmonic oscillator propagated with a time-dependent force, we can rewrite the forward propagator as

$$\hat{G}_L(t) = \hat{T} \exp\left[i \int_0^t f_L(t') \hat{q}(t-t')/\hbar \; dt' \right] \exp[-i\hat{H}_0 t/\hbar] = \exp[i(a_L \hat{q} - b_L \hat{p})] \exp[-i\hat{H}_0 t/\hbar], \tag{A4}$$

where $\hat{T}$ is the time ordering operator, and parameters a_L and b_L are defined as

$$a_L = \frac{1}{\hbar} \int_0^t f_L(t') \cos[\omega_0 (t-t')] \; dt', \tag{A5}$$

$$b_L = \frac{1}{m\omega_0 \hbar} \int_0^t f_L(t') \sin[\omega_0 (t-t')] \; dt'. \tag{A6}$$

Similar relations hold for the backward propagation. Then, making use of the operator identities $\exp(\hat{A}+\hat{B}) = \exp\hat{A} \exp\hat{B} \exp -[\hat{A},\hat{B}]/2$ and $\exp(-i\hat{H}_0 t/\hbar)\hat{\rho}_{eq} \times \exp(i\hat{H}_0 t/\hbar) = \hat{\rho}_{eq}$, we arrive at

$$\rho(q_1, q_2, t) = e^{i(a_L b_L - a_R b_R)/2} \, e^{i(a_L q_1 - a_R q_2)} \times \rho_{eq}(q_1 - b_L, q_2 - b_R). \tag{A7}$$

This result is better expressed in the Wigner representation as

$$W(q,p,t) = \frac{1}{2\pi} \left(\frac{1}{\langle q^2 \rangle \langle p^2 \rangle} \right)^{1/2} \exp\left\{ -\frac{[q - \overline{q(t)}]^2}{2\langle q^2 \rangle} - \frac{[p - \overline{p(t)}]^2}{2\langle p^2 \rangle} + i\phi(t)/\hbar \right\}, \tag{A8}$$

where $\langle q^2 \rangle$ and $\langle p^2 \rangle$ are the equilibrium mean square fluctuations of position and momentum, respectively, and other variables are given as

$$\overline{q(t)} = \int_0^t c_2(t-t') f_+(t') + i c_1(t-t') f_-(t') dt', \tag{A9}$$

$$\overline{p(t)} = m\overline{q(t)}, \tag{A10}$$

and

$$\phi(t) = -\int_0^t U_-(t') dt' + \int_0^t f_-(t') \hat{q}(t') dt'. \tag{A11}$$

Here, $c_2(t)$ and $c_1(t)$ are the real and imaginary parts of the harmonic oscillator correlation function written as

$$c(t) = \hbar[c_1(t) - i c_2(t)] = \frac{\hbar}{2m\omega_0} [\coth(\hbar\beta\omega_0/2)\cos(\omega_0 t) - i \sin(\omega_0 t)]. \tag{A12}$$

Also, $f_+ = f_L + f_R$ and $f_- = f_L - f_R$ are the sum and the difference of the force constants, respectively, and U_- and U_+ are defined in a similar way.

Although the above results are given for a single harmonic oscillator, the generalization to a set of uncoupled harmonic oscillators is straightforward and requires little

modification. A more interesting situation is a two-level oscillator which couples linearly to an infinite set of bath oscillators as described in Eqs. 2.1–(2.3). One can in principle project out the dynamics on the original coordinate of the Brownian oscillator by diagonalizing the force constant matrix of the oscillator-bath potential, given in the mass-scaled coordinates as

$$\mathbf{K}=\begin{pmatrix} \omega_0^2+c_0 & c_1' \ldots c_N' \\ c_1' & \overline{\omega_1^2} \ldots 0 \\ \vdots\vdots & \vdots\vdots \\ c_N' & 0 \ldots \overline{\omega_N^2} \end{pmatrix} \tag{A13}$$

where $c_j'=c_j/\sqrt{\omega_j}$ and $c_0=\Sigma c_j/\omega_j^2$

Evidently, the final expression will retain the same functional form as Eq. (A8) and one simply has to find corresponding expressions for $\langle q^2\rangle$,$\langle p^2\rangle$, and $c(t)$ for the Brownian oscillator. The equilibrium parameters are obtained from the imaginary time path integral formulation, giving

$$\langle q^2\rangle=\sum_n \frac{1}{m\beta}\left(\frac{1}{\mathbf{K}+\Omega_n^2}\right)_{00} = \sum_n \frac{1}{m\beta}\frac{1}{(\Omega_n^2+\omega_0^2)+\Omega_n\tilde{\eta}(\Omega_n)/m}, \tag{A14}$$

$$\langle p^2\rangle=\sum_n \frac{1}{m\beta}\left(\frac{\mathbf{K}}{\mathbf{K}+\Omega_n^2}\right)_{00} = \sum_n \frac{1}{m\beta}\frac{\omega^2+\Omega_n\tilde{\eta}(\Omega_n)/m}{(\Omega_n^2+\omega_0^2)+\Omega_n\tilde{\eta}(\Omega_n)/m}, \tag{A15}$$

where $\Omega_n=2\pi n/\hbar\beta$ and $\tilde{\eta}(\Omega_n)$ is the Laplace transformation of the friction kernel. The real time position–position correlation function can be obtained from linear response theory, giving

$$c_1(t)=\frac{1}{2\pi}\int \coth(\hbar\omega\beta/2)\sin(\omega t)\ \mathrm{Im}\ \chi(\omega)\ d\omega, \tag{A16}$$

$$c_2(t)=\frac{1}{2\pi}\int \cos(\omega t)\ \mathrm{Im}\ \chi(\omega) d\omega. \tag{A17}$$

Here, the linear response function $\chi(\omega)$ is obtained from the analytical continuation of its imaginary correspondence and is explicitly given as

$$\chi(\omega)=\frac{1}{m(\omega_0^2-\omega^2)-i\omega\tilde{\eta}(i\omega)}. \tag{A18}$$

APPENDIX B: MONTE CARLO SAMPLING OF THE GAUSSIAN FORCE

The first step toward our goal is to sample the three terminal points on the trace loop described by the quadratic action

$$\begin{aligned} S(x_1,x_2,x_3)/\hbar &= [S_\beta(x_1,x_2,\beta)-iS_f(x_1,x_3,t)+iS_b(x_2,x_3,t)]/\hbar \\ &= \frac{1}{2}\mathbf{xSx}=\frac{m\omega}{2\hbar\ \sinh(\omega\hbar\beta)}[(x_1^2+x_2^2)-2x_1x_2\cosh(\omega\hbar\beta)] \\ &\quad -i\frac{m\omega}{2\hbar\ \sin(\omega t_f)}[(x_1^2+x_3^2)-2x_1x_3\ \cos(\omega t_f)] \\ &\quad +i\frac{m\omega}{2\hbar\ \sin(\omega t_f)}[(x_2^2+x_3^2)-2x_2x_3\ \cos(\omega t_f)], \end{aligned} \tag{B1}$$

where $\mathbf{x}=(x_1,x_2,x_3)$ is a three-dimensional vector and **S** is a three-dimensional matrix. In this section, a single mode notation is adopted for simplicity unless specified. It is shown in the Appendix of the paper by Cao *et al.*[36] that the three-dimensional complex matrix **S** can be diagonalized by a uniform matrix **U** so that

$$e^{-S/\hbar}=\exp\left[-\frac{1}{2}(\lambda_1y_1^2+\lambda_2y_2^2+\lambda_3y_3^2)/\hbar\right], \tag{B2}$$

where **y** is the transformed terminal coordinates determined by $\mathbf{x}=\mathbf{U}\mathbf{y}$ and the λ's are the eigenvalues, both given in the Appendix of the paper by Cao *et al.*.[36]

Note that the transformation matrix **U** and the eigenvalue λ are complex functions. In order to perform Monte Carlo sampling of a complex Gaussian function $e^{-\lambda y^2/2}$, one introduces a coordinate rotation

$$\eta=ye^{i\theta/2}, \tag{B3}$$

where the rotation angle θ is determined from $\lambda=\rho e^{i\theta}$, so that the new Gaussian function reads

$$e^{-\lambda y^2/2}=e^{-\rho\eta^2}. \tag{B4}$$

Then, any expectation value of y can be expressed as

$$\begin{aligned} \langle f(y)\rangle_\lambda &= \frac{1}{\sqrt{2\pi\lambda}}\int_{-\infty}^{\infty} f(y)e^{-\lambda y^2/2}\,dy \\ &= \frac{1}{\sqrt{2\pi\rho}}\int_{-\infty}^{\infty} f(\eta e^{-i\theta/2})e^{-\rho\eta^2/2}\,d\eta, \end{aligned} \tag{B5}$$

where the functional form of f is assumed regular for the coordinate transformation. This procedure removes the sign problem of any quadratic actions in the Monte Carlo sampling.

The next step is to sample the intermediate time slices of the discretized Feynman path. Given the two end points x_t and x_0 determined from the previous step, we have the real time propagator in the discretized form

$$\langle x_f|e^{-iH_b t/\hbar}|x_0\rangle=\left[\frac{m\omega}{2\pi i\hbar\ \sin(\omega t)}\right]^{P/2}\prod_{n=1}^{P-1}\int dx_n \times\exp\left\{\frac{m\omega i}{2\hbar\ \sin(\omega\epsilon)}\sum_{n=1}^{P}\left[(x_{n-1}^2+x_n^2)-2x_{n-1}x_n\cos(\omega\epsilon)\right]\right\}, \tag{B6}$$

where the subscripts denote the discretized time slice of increment $\epsilon=t_f/P$ and $x_P=x_f$. Introducing the classical trajectory x_{cl} and discretized Fourier modes a_l, one then Fourier decomposes the path as

$$x_n=x_{cl}(t_n)+\sum_{l=1}^{P-1} a_l\ \sin(l\pi n/P), \tag{B7}$$

where the classical solution connecting the two end points is given by

$$x_{cl}(t)=\frac{x_P\ \sin(\omega t)+x_0\ \sin[\omega(t_f-t)]}{\sin(\omega t_f)}, \tag{B8}$$

and the Fourier modes decouple the quadratic action in Eq. (B 6). Consequently, the real time action functional assumes the form

$$S([x_n])=S_{cl}(x_0,x_t;t)+\sum\frac{m}{2}\frac{t_f'}{\hbar}\left\{2[1-\cos(\pi l/P)]\frac{P^2}{t_f'}-\omega'^2\right\}a_l^2/2. \tag{B9}$$

Here, because of the use of the exact quadratic propagator, the parameters t_f' and ω' are the rescaled time and frequency defined by

$$t_f'=t_f\frac{\sin(R)}{R},\qquad \omega'=\omega\frac{1}{\cos(R/2)}, \tag{B10}$$

with $R=t_f\omega/P$. Again, the coordinate rotation on a_n is employed to treat the complex Gaussian width. Similar procedures can be applied to the backward path and, in imaginary time, to the thermal path.

[1] S. A. Rice, Science **258**, 412 (1992).
[2] D. J. Tannor and S. A. Rice, J. Chem. Phys. **83**, 5013 (1985).
[3] W. S. Warren, H. Rabitz, and M. Dahleh, Science **259**, 1581 (1993).
[4] P. Brumer and M. Shapiro, Faraday Disc. Chem. Soc. **82**, 177 (1986).
[5] P. Brumer and M. Shapiro, Annu. Rev. Phys. Chem. **43**, 257 (1992).
[6] B. Kohler, J. Krause, F. Raksi, K. R. Wilson, R. M. Whitnell, V. V. Yakovlev, and Y. J. Yan, Acct. Chem. Res. **28**, 133 (1995).
[7] B. Kohler, V. V. Yakovlev, J. Che, J. L. Krause, M. Messina, K. R. Wilson, N. Schwentner, R. M. Whitnell, and Y. J. Yan, Phys. Rev. Lett. **74**, 3360 (1995).
[8] D. J. Tannor, R. Kosloff, and S. A. Rice, J. Chem. Phys. **85**, 5805 (1986).
[9] R. Kosloff, S. A. Rice, P. Gaspard, S. Tersigni, and D. J. Tannor, Chem. Phys. **139**, 201 (1989).
[10] R. S. Judson and H. Rabitz, Phys. Rev. Lett. **68**, 1500 (1992).
[11] Y. J. Yan, R. E. Gillilan, R. M. Whitnell, K. R. Wilson, and S. Mukamel, J. Phys. Chem. **97**, 2320 (1993).
[12] J. L. Krause, R. M. Whitnell, K. R. Wilson, and Y. J. Yan, in *Femtosecond Chemistry*, edited by J. Manz and L. Wöste (Springer-Verlag, Weinheim, 1995), p. 743.
[13] J. Cao and K. R. Wilson, Phys. Rev. A (submitted).
[14] V. A. Apkarian, C. J. Bardeen, J. Che, B. Kohler, C. C. Martens, M. Messina, K. R. Wilson, V. V. Yakovlev, and R. Zadoyan, in *Ultrafast Phenomena X*, edited by J. Fujimoto, W. Zinth, P. F. Barbara, and W. H. Knox, (Springer-Verlag, Berlin, 1996), p. 219.
[15] C. J. Bardeen, J. C. K. R. Wilson, V. V. Yakovlev, P. Cong, B. Kohler, J. L. Krause, and M. Messina, J. Phys. Chem. (submitted).
[16] C. J. Bardeen, J. Che, K. R. Wilson, V. V. Yakovlev, A. P. Apkarian, C. C. Martens, R. Zadoyan, B. Kohler, and M. Messina, J. Chem. Phys. (submitted).
[17] M. Messina and K. R. Wilson, Chem. Phys. Lett. **241**, 502 (1995).
[18] J. Che, M. Messina, K. R. Wilson, V. A. Apkarian, Z. Li, C. C. Martens, R. Zadoyan, and Y. J. Yan, J. Phys. Chem. **100**, 7873 (1996).
[19] M. Messina, K. R. Wilson, and J. L. Krause, J. Chem. Phys. **104**, 173 (1996).
[20] J. Che, J. L. Krause, M. Messina, K. R. Wilson, and Y. J. Yan, J. Phys. Chem. **99**, 14949 (1995).
[21] J. Cao and K. R. Wilson (1996), J. Chem. Phys. (submitted).
[22] R. P. Feynman and A. R. Hibbs, *Quantum Mechanics and Path Integrals* (McGraw-Hill, New York, 1965).
[23] B. J. Berne, J. Stat. Phys. **43**, 911 (1986).
[24] L. S. Schulman, *Techniques and Applications of Path Integration* (Wiley, New York, 1986).
[25] J. D. Doll and J. E. Gubernatis, *Quantum Simulations of Condensed Matter Phenomena* (World Scientific, Singapore, 1990).
[26] D. Chandler, in *Liquides, Cristallisation et Transition Vitreuse, Les Houches, Session LI*, edited by D. Levesque, J. Hansen, and J. Zinn-Justin (Elsevier, New York, 1991).
[27] M. S. Swanson, *Path Integrals and Quantum Processes* (Academic, San Diego, 1992).
[28] R. W. Zwanzig, J. Stat. Phys. **9**, 215 (1973).
[29] A. O. Caldeira and A. J. Leggett, Ann. Phys. (NY) **149**, 374 (1983).
[30] A. Schmid, J. Low. Temp. Phys. **49**, 609 (1982).
[31] E. Pollak, J. Chem. Phys. **85**, 865 (1986).
[32] C. H. Mak and D. Chandler, Phys. Rev. A **44**, 2352 (1991).
[33] R. Egger and C. H. Mak, J. Chem. Phys. **99**, 2541 (1993).
[34] D. Makarov and N. Makri, Phys. Rev. A **48**, 3626 (1993).
[35] D. Makarov and N. Makri, Chem. Phys. Lett. **221**, 482 (1994).
[36] J. Cao, L. W. Ungar, and G. A. Voth, J. Chem. Phys. **104**, 4189 (1996).
[37] Y. J. Yan and S. Mukamel, J. Chem. Phys. **89**, 5160 (1988).
[38] Y. Tanimura and S. Mukamel, Phys. Rev. E **47**, 118 (1993).
[39] J. Cao and G. A. Voth (in preparation).
[40] Y. J. Yan and S. Mukamel, J. Chem. Phys. **88**, 5735 (1988).
[41] B. J. Berne and D. Thirumalai, Annu. Rev. Phys. Chem. **37**, 401 (1986).
[42] M. Berman and R. Kosloff, Comput. Phys. Commun. **63**, 1 (1991).
[43] E. J. Heller, J. Chem. Phys. **62**, 1544 (1975).
[44] E. J. Heller, Acc. Chem. Res. **14**, 368 (1981).
[45] G. Campolieti and P. Brumer, Phys. Rev. A **50**, 997 (1994).
[46] J. Cao and G. A. Voth, J. Chem. Phys. **104**, 273 (1996).
[47] J. Cao and G. A. Voth, J. Chem. Phys. **100**, 5106 (1994).
[48] R. M. Whitnell, K. R. Wilson, Y. J. Yan, and A. H. Zewail, J. Mol. Liq. **61**, 153 (1994).